23rd ABCM International Congress of Mechanical Engineering
December 6-11, 2015, Rio de Janeiro, RJ, Brazil

SENSITIVITY ANALYSIS OF A HORIZONTAL STATIONARY HEAT TRANSFER SLUG FLOW MODEL ON THE ELONGATED BUBBLE VELOCITY

Carlos L. Bassani, langebassani@gmail.com
Fernando H. G. Pereira, fernandopereira@alunos.utfpr.edu.br
Fausto A. A. Barbuto, fausto_barbuto@yahoo.ca
Rigoberto E. M. Morales, rmorales@utfpr.edu.br
Multiphase Flow Center (NUEM), Postgraduated Program in Mechanical and Materials Engineering (PPGEM), Federal University of Technology – Paraná (UTFPR) – Av. Sete de Setembro, 3165 - Rebouças CEP 80230-901 - Curitiba - PR - Brasil

Abstract. *The two-phase slug flow pattern occurs over a wide range of gas and liquid flow rates and is frequently found in oil and gas offshore transportation operations. Due to the high complexity of this kind of multiphase flow, several experimental works attempted to model some important parameters such as the slug frequency and the elongated bubble translational velocity. The experimental correlations that arose from such works are widely used today on stationary slug flow simulators so as to provide mathematical closure to several models, as the one that will be presented here. Yet, those correlations were developed under different experimental conditions, where the pipe geometry, the fluid properties and even the measurement techniques widely affect the shape and/or the extrapolated accuracy of those experimental correlations. Therefore, the present work presents a sensitivity analysis of a heat transfer model for stationary gas-liquid slug flows in horizontal pipes in terms of the chosen elongated bubble velocity correlation. The sensitivity analysis for the pressure and temperature gradients predictions is shown here, as well as for the two-phase flow heat transfer coefficient and for the length of the slug flow structures.*

Keywords: *multiphase flow, slug flow, heat transfer, sensitivity analysis.*

1. INTRODUCTION

Multiphase flows are widely encountered in nature, for example when solid sediments are transported by river streams, and in industrial applications, notably in boiling/condensing flows and on mixture transportations. In gas-liquid two-phase flows several flow patterns – that is, the shapes assumed by the distribution of the gas-liquid interfaces – may occur. Slug flow is one of those patterns, and it occurs for wide liquid and gas flow rate ranges and is commonly encountered during oil and gas transportation operations. This pattern is characterized by the intermittent succession of an elongated bubble flowing over a liquid film and a liquid slug that may or not contain dispersed bubbles. Those two different regions form that what is known as a *unit cell* and presents different velocities, lengths and phase fractions in space and time.

Many authors attempted to model the liquid-gas slug flow phenomena through different approaches, be they either stationary or transient. The main objectives of those approaches were to predict both the pressure drop, an important parameter in the design and operation of production facilities and the slug flow region lengths and/or frequency, which relate to pipeline vibration. The importance in predicting phase fractions and distributions when mixture separation is required for posterior pumping operations is also noteworthy. Less studied due to its highly complex modelling, the mixture temperature distribution is also very important in the prediction of wax and hydrates deposition regarding flow assurance analyses. Earlier approaches used a stationary one-dimensional modelling, predicting the mass and momentum conservations of the unit cell along the pipe (Medina *et al*., 2010; Dukler and Hubbard, 1975; Fernandes *et al*., 1983; Taitel and Barnea, 1990a). With the evolution of the digital computers after the 1990's, some transient approaches began to appear, such as the slug tracking lagrangian method (Barnea and Taitel, 1993; Nydal and Banerjee, 1995; Perea Medina *et al*., 2015; Rodrigues, 2009), obtaining more flow details such as the coalescence phenomenon and the intermittent distribution of the main slug flow hydrodynamic parameters over space and time.

Either approach has its strengths and weaknesses. The stationary models are very stable and capable of predicting the mean parameters of the slug flow fairly well, but they do not consider their distribution. The transient approaches do provide this kind of information, but at a higher computational cost nevertheless and are show numerical instabilities and divergences more frequently. Regardless the model, in a stronger or weaker way they depend on some kind of closure relationships obtained from experimental data. Thus, many authors developed closure relationships based on experimental data, notably for the bubble nose translational velocity (Bendiksen, 1984; Nicklin *et al*., 1962; Petalas and Aziz, 1998), for the slug flow frequency (Gregory and Scott, 1969; Heywood and Richardson, 1979; Zabaras, 2000) and for the slug region liquid holdup (Andreussi *et al*., 1993; Barnea and Brauner, 1985; Gregory *et al*., 1978). Regardless their broad use, the precision range of those closure relationships is strictly related to the experimental setup and measuring conditions, such as the properties of the phases and pipe diameter, inclination and developing length. Moreover, the type of gas and liquid mixing apparatus used (e.g., parallel plates or porous medium) and the pipeline structural rigidity are related to the stratified to slug flow transition and may be one of the causes of the high discrepancies between the different slug flow frequency correlations, as reported by Antunes *et al*. (2014).

Having all those issues considered, the present work brings forth analyses on such variations between several closure relationships found in the literature and on the propagation of uncertainties that arose when using a stationary slug flow model. This work is part of a series of validations of the stationary slug flow simulator developed at the NUEM/PPGEM/UTFPR facilities, capable of predicting pressure and temperature drops, the two-phase heat transfer coefficient and the characteristic lengths, velocities and phase fractions distributions along the pipeline. The focus of the present work is a sensitivity analysis on the bubble nose translational velocity closure relationships encountered on the literature, fixing the other required parameters during the simulations.

2. MATHEMATICAL MODEL

The mathematical model is based on the unit cell mass, momentum and energy conservation equations in their integral form applied to the deformable control volume shown in Fig. 1.The main hypotheses assumed during modelling are: (i) stationary, periodic, horizontal and one-dimensional slug flow, (ii) incompressible liquid and ideal gas, (iii) uniform velocity profile in each unit cell structure, (iv) constant phase fractions in each unit cell region, (v) negligible shear stresses in the elongated gas bubble and at the phases' interfaces, (vi) negligible gas momentum and internal energy when compared to the liquid phase due to the lower specific mass and heat of the gaseous phase, (vii) negligible viscous energy dissipation, (viii) negligible kinetic energy compared to the internal energy, (ix) negligible heat transfer between the dispersed bubbles and the liquid slug and (x) constant external temperature boundary condition.

The liquid and gas mass conservation is applied to the control volume CV1 of Fig. 1 in order to predict the liquid and gas velocities in the elongated bubble region, as previously done by Taitel and Barnea (1990a):

$$U_{LB} = U_T - \left(U_T - U_{LS}\right)\frac{R_{LS}}{R_{LB}} \quad ; \quad U_{GB} = U_T - \left(U_T - U_{GS}\right)\frac{\left(1-R_{LS}\right)}{R_{GB}} \tag{1}$$

where R is the phase fraction and U the velocity. The subscripts relate to the liquid in the slug (*LS*), the liquid in the film (*LB*), the gas in the elongated bubble (*GB*) and the dispersed gas bubbles in the liquid slug (*GS*). The liquid slug velocity U_{LS} can be found assuming constant superficial mixture velocity J through the pipe cross sectional area for any unit cell region flowing through it (Shoham, 2006):

$$U_{LS} = \frac{J - U_{GS}\left(1-R_{LS}\right)}{R_{LS}} \tag{2}$$

Finally, the velocity of the dispersed bubbles in the slug region can be approximated by the mixture velocity, $U_{GS} \approx J$ (Harmathy, 1960). Once all the velocities are specified, the pressure drop in the unit cell can be estimated by applying the momentum balance to the control volume CV2 of Fig. 1:

$$-\left.\frac{dP}{dz}\right|_U = \frac{\tau_{LS}\pi D L_S + \tau_{LB} S_{LB} L_B}{A L_U} + \frac{\Delta P_{mix}}{L_U} \tag{3}$$

where D is the pipe diameter, S is the wetted perimeter, L is the length and A is the cross sectional area. The subscript U refers to the unit cell. The shear stresses τ due to the phase friction on the wall can be estimated by assuming single-phase liquid flow throughout each unit cell structure using the specific hydraulic diameter and Reynolds number. The pressure drop in the mixture zone is due to the sudden expansion of the liquid-occupied area behind the elongated bubble and can be modeled as $\Delta P_{mix} = K\rho_L\left(U_{LB} - U_T\right)^2/2$, similarly to Cook and Behnia (2000), where U_T is the elongated bubble translational velocity and K is a constant that depends on the expansion area ratio, herein approximated as 0.4. Equation (3) needs the slug and elongated bubble length, which can be estimated by Taitel and Barnea's (1990b) model for the bubble profile:

$$\frac{dH_{LB}}{dz}=\frac{\dfrac{\tau_{LB}S_{LB}}{AR_{LB}}-\dfrac{\tau_{GB}S_{GB}}{AR_{GB}}-\tau_i S_i\left(\dfrac{1}{AR_{LB}}+\dfrac{1}{AR_{GB}}\right)+\left(\rho_L-\rho_G\right)g\sin\gamma}{\left(\rho_L-\rho_G\right)g\cos\gamma-\rho_L\dfrac{\left(U_{LB}-U_T\right)^2}{R_{LB}}\dfrac{dR_{LB}}{dH_{LB}}-\rho_G\dfrac{\left(U_{GB}-U_T\right)^2}{R_{GB}}\dfrac{dR_{LB}}{dH_{LB}}} \tag{4}$$

where H_{LB} is the liquid film height, z is the axial coordinate and γ is the pipe inclination. Equation (4) can be integrated until convergence with the unit cell mass conservation:

$$\frac{L_U\left(U_{LS}R_{LS}-j_L\right)}{U_T}=R_{GB}L_B-L_B\left(1-R_{LS}\right) \tag{5}$$

where the *LHS* of eq. (5) does not change during the integration process, whereas the *RHS* does. The bubble length can be determined as the sum of all dz increments in the integration and the mean bubble void fraction as $R_{GB}=1-\left(H_{LB}/D\right)$. The unit cell length is estimated with the frequency and the bubble nose translational velocity obtained with closure relationships, and is expressed as $L_U=U_T/freq$.

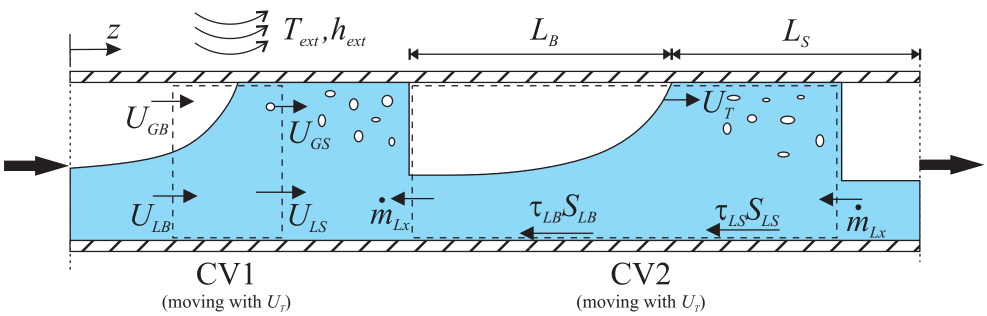

Figure 1. Control volumes for conservation equations.

The energy conservation equation is applied to the control volume CV2 of Fig. 1 considering the different heat change rates in the slug and film regions, due to their characteristic Reynolds numbers and wetted perimeter. The axial heat transfer due to the mass exchange between two adjacent unit cells, i.e., the scooping phenomenon (Shoham, 2006), is also considered in the model. Thus, the following expression for the mixture temperature distribution comes:

$$T_{m(z)}=T_W+\left(T_{mi}-T_W\right)\exp\left(-\left[\frac{h_{LB}S_{LB}L_B+h_{LS}S_{LS}L_S-\kappa\dot{m}_{Lx}C_L}{\rho_L R_{LU}AU_T L_U C_L}\right]z\right) \tag{6}$$

where, T_W is the wall temperature, T_{mi} is the mixture temperature at the pipe inlet, h is the heat transfer coefficient, S is the wetted perimeter, R_{LU} is the mean liquid holdup in the unit cell, ρ_L and C_L are the liquid density and specific heat, respectively, κ is a dimensionless parameter defined for the model, $\dot{m}_{Lx}$ is the scooping mass flow rate and z is the axial pipe coordinate. Table 1 defines the parameters used in eq. (6) that have yet to be specified.

Table 1. Definition of the main parameters for the unit cell energy conservation equation.

$\dot{m}_{Lx}=\rho_L R_{LB}A(U_{LB}-U_T)=\rho_L R_{LS}A(U_{LS}-U_T)$	(7)	$\kappa=\left[\exp\left(\dfrac{h_{LB}S_{LB}L_B}{\dot{m}_{LB}C_L}\right)-\exp\left(-\dfrac{h_{LS}SL_S}{\dot{m}_{LS}C_L}\right)\right]$	(8)
$\dot{m}_{LS}=\rho_L R_{LS}A\left(U_T+U_{LS}\right)$	(9)	$\dot{m}_{LB}=\rho_L R_{LB}A\left(U_T+U_{LB}\right)$	(10)
$T_W=T_W^{LB}\dfrac{L_B}{L_U}+T_W^{LS}\dfrac{L_S}{L_U}$	(11)	$h_\phi^O=\left[\dfrac{D}{D_{ext}h_{ext}}+\dfrac{D\ln\left(D_{ext}/D\right)}{2k}+\dfrac{1}{h_\phi}\right]^{-1}$	(12)
$T_W^\phi=T_m+\dfrac{h_\phi^O}{h_\phi}\dfrac{D}{D_{ext}}\left(T_{ext}-T_m\right)$	(13)	$R_{LU}=R_{LB}\dfrac{L_B}{L_U}+R_{LS}\dfrac{L_S}{L_U}$	(14)

Where: $\phi=LB,LS$

Comparing the mixture temperature distribution to a simple homogeneous model, the two-phase flow heat transfer coefficient can be expressed as:

$$h_{TP} = \left(h_{LB} \frac{S_{LB}}{S} \frac{L_B}{L_U} + h_{LS} \frac{S_{LS}}{S} \frac{L_S}{L_U} - \frac{\kappa \dot{m}_{Lx} C_L}{S L_U} \right) \frac{j_L}{R_{LU} U_T} \tag{15}$$

where j_L is the liquid superficial velocity.

3. CLOSURE RELATIONSHIPS

The mathematical model presented in the previous section is able to estimate the pressure and temperature distributions as well as the characteristic velocities, lengths and phase fractions in the elongated bubble and liquid slug regions. Nevertheless, the number of variables exceeds the number of equations, thus making the system undefined. Therefore, some variables must be estimated by experimental closure relationships.

A first assumption is made for the liquid phase fraction in the slug region, R_{LS}, needed in eqs. (1), (2), (5), (7), (9) and (14). For horizontal slug flow, the dispersed bubble entrainment in the liquid slug is low or even zero for small mixture velocities, with $Fr = J / \sqrt{gD} \leq 3.5$ (Rogero, 2009). Preliminary simulations that will not be shown in the present work presented a small sensibility of the model with regard to the liquid slug holdup, and therefore this latter will be fixed and calculated by the Andreussi *et al.* (1993) correlation.

The unit cell length, needed by eqs. (3), (5), (6), (15), (11) and (14), is predicted by both frequency and bubble nose translational velocities closure relationships, as shown in the previous section. The frequency correlations proposed in the literature show a large discrepancy amongst themselves, as pointed by Antunes *et al.* (2014). Preliminary simulations showed a large sensitivity of the bubble and slug lengths with regard to the frequency used as an input parameter and obtained by correlations. Yet the L_S/L_U ratio estimated by the Taitel and Barnea (1990a) methodology remains similar for the different correlations, therefore this sensitivity does not propagate to the pressure, temperature and heat transfer coefficient, eqs. (3), (6) and (15), respectively. Further analysis about the sensitivity of the frequency closure relationships on the lengths of the structures in a unit cell could be made, but the present work focus on the pressure and temperature drops. Thus, the frequency throughout this work is calculated by the Heywood and Richardson (1979) correlation.

Table 2. Experimental closure relationships for the elongated bubble translational velocity.

Author(s)	C_0	C_1	*Re*	Geometry
Dukler and Hubbard (1975)	$1.022 + 0.021\ln(\mathrm{Re}_j)$	-	30000 to 400000	Horizontal
Ferré (1979)	1.10 $Fr_j \leq 2.26$ 1.30 $2.26 < Fr_j < 8.28$ 1.02 $Fr_j \geq 8.28$	0.44 $Fr_j \leq 2.26$ 0 $2.26 \leq Fr_j < 8.28$ 3 $Fr_j \geq 8.28$	-	Horizontal
Bendiksen (1984)	$1.05 + 0.15(\mathrm{sen}\gamma)^2$ $Fr_{j_L} < 3.5$ 1.2 $Fr_{j_L} \geq 3.5$	$0.54\cos\gamma + 0.35\mathrm{sen}\gamma$ $Fr_{j_L} < 3.5$ $0.35\mathrm{sen}\gamma$ $Fr_{j_L} \geq 3.5$	-	Horizontal & Vertical
Dukler *et al.* (1985)	1.225	-	> 8000	Horizontal & Vertical
Théron (1989)	$1.3 - \frac{0.23}{\Gamma} + 0.13(\mathrm{sen}\gamma)^2$	$\left(-0.5 + \frac{0.8}{\Gamma}\right)\cos\gamma + 0.35\mathrm{sen}\gamma$	-	Horizontal & Vertical
Manolis (1995)	1.033 $Fr_j < 2.86$ 1.216 $Fr_j \geq 2.86$	0.477 $Fr_j < 2.86$ 0 $Fr_j \geq 2.86$	-	Horizontal
Woods and Hanratty (1996)	1.1 $Fr_j < 3.1$ 1.2 $Fr_j \geq 3.1$	0.52 $Fr_j < 3.1$ 0 $Fr_j \geq 3.1$	-	Horizontal
Petalas and Aziz (1998)	$\frac{1.64 + 0.12\mathrm{sen}\gamma}{\mathrm{Re}_j^{0.031}}$	-	-	Horizontal & Vertical

Where: $\mathrm{Fr}_{j_L} = \frac{j_L}{\sqrt{gD}}$; $\Gamma = 1 + \left(\frac{\mathrm{Fr}_j}{\mathrm{Fr}_{Crit}}\cos\gamma\right)$, with $Fr_{crit} = 3.5$; and $\mathrm{Re}_j = \frac{\rho_L jD}{\mu_L}$.

Equations (1), (4), (5), (6), (15), (7), (9) and (10) require the determination of the bubble nose translational velocity, U_T. Since the control volumes for determining the mass, momentum and energy conservation equations travel along the pipe with this velocity, U_T thus becomes one of the most sensitive parameters of the model. Fortunately, this parameter has been largely studied by many authors and expressing it as a linear function of the superficial mixture velocity (Nicklin *et al*., 1962) is widely accepted in the literature:

$$U_T = C_0 J + C_1 \sqrt{gD} \tag{16}$$

Equation (16) shows that the elongated bubble translational velocity can be correlated to two different phenomena: the pushing inertia of the mixture, first term of the RHS, and the drift velocity between the liquid and gas phases, second term of the RHS. The constants C_0 and C_1 were experimentally measured by many authors and diverge by approximately ±10%, as will be shown later in the section dedicated to the sensitivity analysis. Table 2 presents a summary of some literature works that focused on the estimation of these constants. There is some debate about the drift velocity in horizontal slug flows, and while some authors (Dukler *et al*., 1985; Petalas and Aziz, 1998) claim that this term is null since there are no thrust forces governing the phenomenon, other researchers (Bendiksen, 1984; Dukler and Hubbard, 1975; Ferré, 1979; Manolis, 1995; Théron, 1989; Woods and Hanratty, 1996) defend that this phenomenon still exists due to the difference between the hydraulic pressure columns in the bubble rear and front, i.e., due to the elongated bubble curved shape.

Finally, some single-phase flow correlations are used to predict the friction factor and the heat transfer coefficient of each unit cell structure, i.e., elongated bubble, liquid slug and liquid film. A simple Blasius-type correlation is used to predict the friction factor, whereas the Gnielinski (1976) correlation is used to calculate the heat transfer coefficient. As those are single-phase flow correlations that were widely validated by experiments, they will remain fixed throughout the simulations.

The present work focus on the sensitivity analysis of the stationary model for different elongated bubble velocity closure relationships, fixing the other closure relationships as specified in this section.

4. SENSITIVITY ANALYSIS

The sensitivity analysis was carried out so as to study the propagation of uncertainties during the simulation due to the differences between the several correlations for U_T found in literature. Since there is not a unique correlation for estimating the parameters C_0 and C_1 of eq. (16), which are strictly related to the measurement conditions and experimental setup, one cannot simply accept or write off any closure relationship. All the studies presented in Table 2 were developed for fluids with similar properties (usually air and water) and similar pipe geometries (1- or 2-inch IDs and at least horizontal inclinations). Yet the correlations have similar application ranges, their results differ and this difference is carried to the simulation. Due to the iterative calculation process for the prediction of the elongated bubble shape, eq. (4), it was chosen to make the propagation of uncertainties numerically instead of analytically.

The simulations were conducted so that the experimental measurements of Lima (2009) could be reproduced. The experiments of Lima (2009) were carried out with an air-water warm mixture flowing through a 52-mm ID (54-mm OD) copper pipe. The mixture was cooled by a water stream flowing concurrently through an outer annular space at a known flow rate. The 6-m length test section is followed by a glass window that allows flow visualization, so as to make sure that slug flow pattern existed for all measured cases. The external heat transfer coefficient h_{ext} was estimated by the Gnielinski (1976) correlation based on the mean velocity of the cold water and the hydraulic diameter of the annulus. The external temperature was approximated as an average between the inlet and the outlet temperature of the coolant medium.

The experimental data measured by Lima (2009) covered a range of gas and liquid superficial velocities of $0.58 \le j_L \le 1.93$ m/s and $0.22 \le j_G \le 0.79$ m/s and an outlet pressure within the $135.1 \le P_{exit} \le 179.4$ kPa range. The external and inlet temperatures varied between $283.1 \le T_{ext} \le 288.1$ K and $307.7 \le T_{mi} \le 318.7$ K, respectively, for all the experimental measurements, whereas the external heat transfer coefficient varied within the $1525 \le h_{ext} \le 2620$ W/m^{2}K range.

All the experimental cases measured by Lima (2009) were reproduced by the simulator here presented for the eight (8) different bubble velocity closure relationships in Table 2. A total of 92% of the simulations converged, i.e., only two out of the 25 cases did not converge due to numerical instabilities that sprang from the integration of eq. (4), that is, instabilities introduced by the prediction of the elongated bubble length. Those two cases have high j_L/j_G ratios.

The results from the simulations were compared with the experimental data obtained by Lima (2009) in order to validate the simulator. Since Lima (2009) measured only pressure and temperature gradients and heat transfer coefficients, the hydrodynamic parameters such as bubble velocities and characteristic lengths were not validated for these simulations. The results lied within a ±30% range for temperature gradient and heat transfer coefficient and within a ±20% range for the pressure gradient, in agreement with the accuracy shown by other slug flow models from the literature. Plots will not be shown here since that is not the objective of the present work.

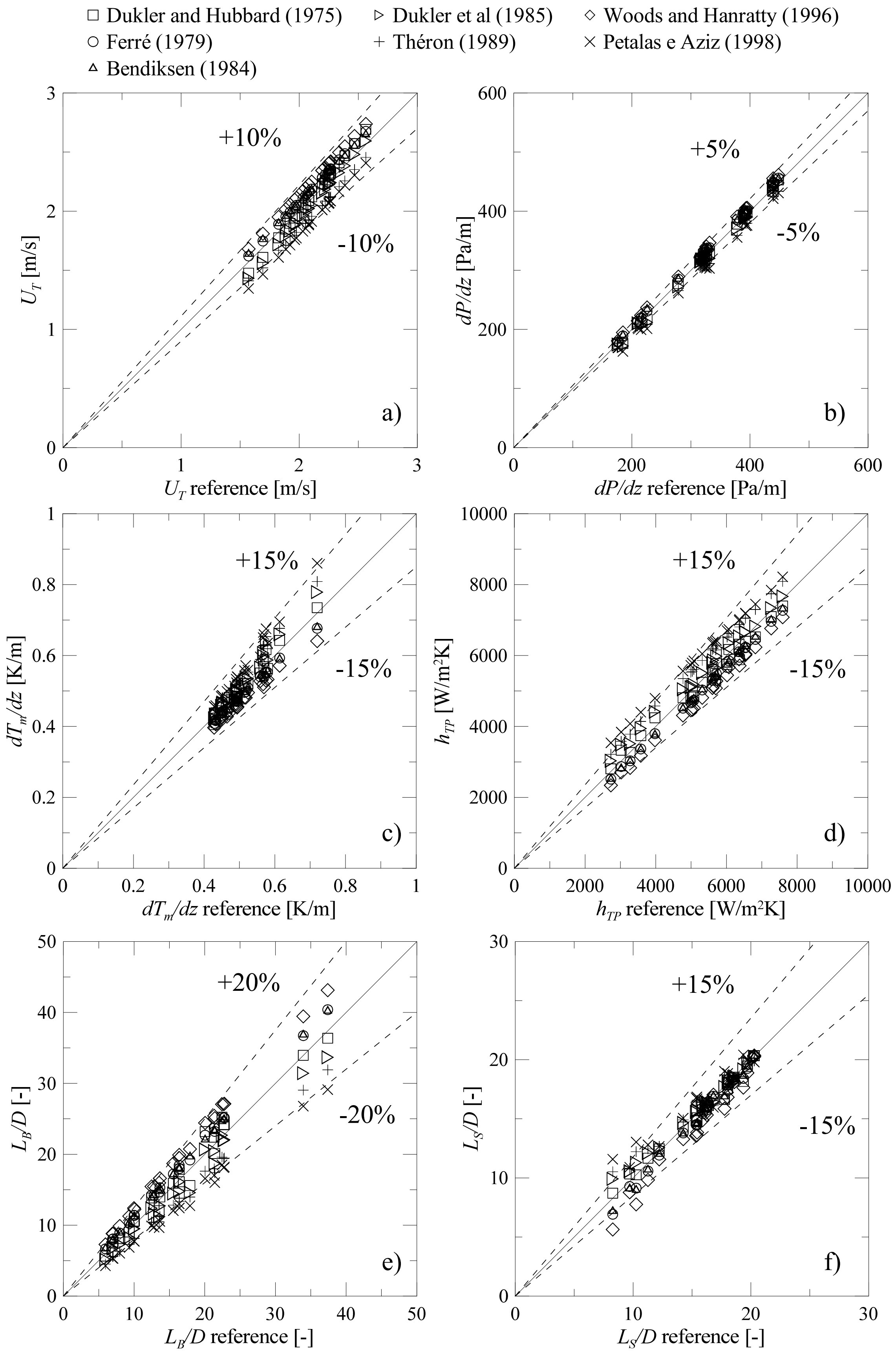

Figure 2. Numerical simulations plotted against a reference simulation with Manolis (1995) for: a) elongated bubble translational velocity, b) pressure gradient, c) temperature gradient, d) two-phase flow heat transfer coefficient, e) dimensionless elongated bubble length and f) dimensionless slug length.

Once the simulator has been validated, it became possible to analyze the model and infer its sensitivity. Figure 2 presents the results for the eight (8) different U_T correlations. Since the objective is to compare the simulations in order to study the propagation of uncertainties due to the U_T input differences a reference simulation is plotted on the *x*-axis. The simulation with Manolis' (1995) correlation was chosen as it showed a better data distribution trend around the 45-degree (that is, the bisector line) compared to the others, thus centralizing graphics of Fig. 2 and simplifying their interpretation.

Figure 2a shows the differences in U_T prediction for the several correlations in Table 2. The plotted points distribute within a ±10% range, showing a very good agreement between them when it comes to slug flow. Figures 2b-f present the range of the other parameters of interest that remained within a range of ±5% for the pressure gradient (Fig. 2b); ±15% for the temperature gradient, the two-phase flow heat transfer coefficient and the slug length (Figs. 2c,d,f); and ±20% for the bubble length. Therefore, one can state that the bubble length is the most sensitive parameter on U_T prediction. These differences are related to the sensitivity of Taitel and Barnea's (1990b) bubble profile model, where the bubble length is calculated by the integration of eq. (4) until convergence with eq. (5) is achieved. Yoshizawa (2005) provides more information about this kind of integration sensitivity. The pressure and temperature gradients are not significantly affected even when the uncertainties on the bubble length prediction amplify, thus allowing for the conclusion that pressure and temperature are, respectively, parameters with low and medium sensitivity on U_T prediction. Those usually are the main parameters of interest in facilities' design and operation, especially when it comes to hydrate formation prediction and other flow assurance issues.

Prior to extending the sensitivity analysis from a qualitative to a quantitative approach, the percentage variation amplitude of a parameter ψ between the simulations done for the *i* different closure relationships must be defined:

$$\delta\psi_{(\%)} = \frac{\max\psi_i - \min\psi_i}{\max\psi_i}(100\%) \tag{17}$$

Moreover, the $\delta\psi_{(\%)}$ parameter can be normalized by the amplitude of the varying parameter U_T:

$$\overline{\delta\psi} = \frac{\delta\psi_{(\%)}}{\delta U_{T(\%)}} \tag{18}$$

The normalized parameter $\overline{\delta\psi}$ represents the amplification or damping of the variation amplitude of the parameter ψ between the simulations using the *i* different closure relationships in comparison with the variation amplitude between these U_T closure relationships. Therefore, when $\overline{\delta\psi} = 1$, there is only propagation of uncertainties, without amplification or damping. For $\overline{\delta\psi} > 1$, there is amplification of U_T uncertainty, showing that the parameter ψ is sensible on the prediction of U_T. For $\overline{\delta\psi} < 1$, there is damping of U_T uncertainty, thus showing a smaller sensitivity of the parameter ψ on the prediction of U_T. The degree of sensitivity is related to the $\overline{\delta\psi}$ module. As an example, for $\overline{\delta\psi} = 2$ or $\overline{\delta\psi} = 0.5$, the initial uncertainty on the prediction of U_T is amplified/damped during the simulation by the double/half for the parameter ψ, respectively.

Table 3 presents statistical analyses for the $\delta\psi_{(\%)}$ and $\overline{\delta\psi}$ parameters for the same physical quantities as before. Actually, Table 3 is a quantitative resume of Fig. 2 showing the mean, maximum and minimum propagation of uncertainties of each ψ parameter, as well as its standard deviation. It is important to observe that the $\delta\psi_{(\%)}$ parameter represents the double of the error lines in Fig. 2 (dashed lines). The most sensitive parameter was the elongated bubble length, with an uncertainty amplifying factor of ≈2.4, whereas the less sensitive parameter was the pressure gradient, with an uncertainty damping factor of ≈0.5.

Table 3. Sensitive analysis on the elongated bubble translational velocity.

$\delta\psi_{(\%)}\left(\overline{\delta\psi}\right)$	U_T	dP/dz	dT_m/dz	h_{TP}	L_S/D	L_B/D
Average	15.1 (1)	7.9 (0.51)	14.9 (0.98)	20.8 (1.37)	13.0 (0.85)	36.1 (2.41)
Standard deviation	2.0 (0)	3.5 (0.16)	4.1 (0.22)	5.4 (0.29)	12.4 (0.77)	2.9 (0.27)
Maximum	20.0 (1)	16.5 (0.83)	25.5 (1.53)	33.8 (2.03)	51.2 (3.08)	41.3 (2.90)
Minimum	12.1 (1)	3.1 (0.25)	10.0 (0.69)	13.7 (0.94)	1.3 (0.08)	31.6 (1.93)

5. CONCLUSIONS

The present work carried out a sensitivity analysis of a stationary heat transfer model for gas-liquid horizontal slug flows, focusing on the influence of several experimental relationships for the elongated bubble translational velocity. The model was briefly presented, emphasizing the benchmarking of the experimental correlations used in the sensitivity analysis. Regardless the low discrepancies shown by several correlations, in order of ±10%, those uncertainties are propagated by the simulator when one correlation is accepted as input. Due to the model's iterative nature, studying the uncertainties propagation by an analytical analysis is not trivial. Thus, this study on the propagation of the uncertainties was achieved by numerical simulations for different elongated bubble velocity closure relationships found in the literature, fixing the other required input parameters. It was found that the most sensitive parameter was the elongated bubble length, which favours the amplification of the uncertainties for a factor of 2.4, whereas the least sensitive parameter was the pressure gradient, with a damping factor of 0.5. The other analyzed parameters, namely the temperature gradient, the two-phase heat transfer coefficient and the slug length, remained between those boundaries. Future analyses might be made for the other input parameters that come from experimental correlations, such as the slug flow frequency and the liquid slug aeration.

6. ACKNOWLEDGEMENTS

The authors acknowledge the financial support from ANP and FINEP through the Human Resources Program to oil and gas segment PRH-ANP (PRH 10 - UTFPR), from TE / CENPES / PETROBRAS and from the National Council for Scientific and Technological Development (CNPq).

7. REFERENCES

Andreussi, P., Bendiksen, K.H., Nydal, O.J., 1993. Void distribution in slug flow. Int. J. Multiph. Flow. doi:10.1016/0301-9322(93)90045-V

Antunes, M.M., Cozin, C., Barbuto, F.A.A., Morales, R.E.M., Rodrigues, H.T., 2014. Analysis of Slug Frequency Correlations for Two-Phase Gas-Liquid Horizontal Slug Flow, in: 4th Joint US-European Fluids Engineering Division Summer Meeting Collocated with the ASME 2014 12th International Conference on Nanochannels, Microchannels, and Minichannels. Chicago.

Barnea, D., Brauner, N., 1985. Holdup of the liquid slug in two phase intermittent flow. Int. J. Multiph. Flow. doi:10.1016/0301-9322(85)90004-7

Barnea, D., Taitel, Y., 1993. A model for slug lenght distribution in gas-liquid slug flow. Int. J. Multiph. Flow 19 (5), 639–649.

Bendiksen, K.H., 1984. An experimental investigation of the motion of long bubbles in inclined tubes. Int. J. Multiph. Flow 10, 467–483.

Cesar D. Perea Medina, Cozin, C., Morales, R.E.M., Junqueira, S.L.M., 2010. Hydrodynamics and heat transfer simulation for two-phase intermittent flow in horizontal pipes, in: 13th Braz. Congr. of Therm. Sci. and Eng. Uberlândia, Brazil.

Cook, M., Behnia, M., 2000. Pressure drop calculation and modelling of inclined intermittent gas-liquid flow. Chem. Eng. Sci. 55, 4699–4708. doi:10.1016/S0009-2509(00)00065-8

Dukler, A.E., Hubbard, M.G., 1975. Model for gas-liquid slug flow in horizontal and near horizontal tubes. Ind. Eng. Chem. Fundam. 14, 337–347. doi:10.1021/i160056a011

Dukler, A.E., Moalem Maron, D., Brauner, N., 1985. A physical model for predicting the minimum stable slug length. Chem. Eng. Sci. doi:10.1016/0009-2509(85)80077-4

Fernandes, R.C., Semiat, R., Dukler, A.E., 1983. Hydrodynamic model for gas-liquid slug flow in vertical tubes. Aiche J. 29, 981–989. doi:10.1002/aic.690290617

Ferré, D., 1979. Ecoulements diphasiques a poches en conduite horizontale. Rev. Inst. Fr. Pet. 34, 113–142.

Gnielinski, V., 1976. New equations for heat and mass transfer in turbulent pipe and channel flow. Int. Chem. Eng. 16, 359–368.

Gregory, G.A., Nicholson, M.K., Aziz, K., 1978. Correlation of the liquid volume fraction in the slug for horizontal gas-liquid slug flow. Int. J. Multiph. Flow. doi:10.1016/0301-9322(78)90023-X

Gregory, G.A., Scott, D.S., 1969. Correlation of liquid slug velocity and frequency in horizontal cocurrent gas-liquid slug flow. AIChE J. 15, 933–935. doi:10.1002/aic.690150623

Harmathy, T.Z., 1960. Velocity of large drops and bubbles in media of infinite or restricted extent. AIChE J. 6, 281–288. doi:10.1002/aic.690060222

Heywood, N.I., Richardson, J.F., 1979. Slug flow of air-water mixtures in a horizontal pipe: Determination of liquid holdup by γ-ray absorption. Chem. Eng. Sci. doi:10.1016/0009-2509(79)85174-X

Lima, I.N.R.C., 2009. Estudo Experimental da Transferência de Calor no Escoamento Bifásico Intermitente Horizontal. Universidade Estadual de Campinas, São Paulo, Brazil.

Manolis, I.G., 1995. High Pressure Gas-Liquid Slug Flow. Imperial College of Science, Technology & Medicine, UK.

Nicklin, D.J., Wilkes, M.A., Davidson, J.F., 1962. Two-Phase Flow in Vertical Tubes, in: Transactions of the Institution of Chemical Engineers.

Nydal, O.J., Banerjee, S., 1995. Objected oriented dynamic simulation of slug flow, in: 2nd Int. Conf. of Multiphase Flow. Kyoto, pp. Vol.2, IF2_7–14.

Perea Medina, C.D., Bassani, C.L., Cozin, C., Barbuto, F.A.A., Junqueira, S.L.M., Morales, R.E.M., 2015. Numerical simulation of the heat transfer in fully developed horizontal two-phase slug flows using a slug tracking method. Int. J. Therm. Sci. 88, 258–266. doi:10.1016/j.ijthermalsci.2014.05.007

Petalas, N., Aziz, K., 1998. A mechanistic model for multiphase flow in pipes, in: 49th Annual Technical Meet. of Petroleum Soc. of the Can. Ins. of Min., Metallurgy & Petroleum. Calgary, Canada.

Rodrigues, H.T., 2009. Simulação numérica do escoamento bifásico líquido-gás no padrão de golfadas utilizando um modelo lagrangeano de seguimento de pistões. Universidade Tecnológica Federal do Paraná.

Rogero, E.C., 2009. Experimental Investigation of Developing Plug and Slug Flows. Tecnhische Universität München.

Shoham, O., 2006. Mechanistic modeling of gas-liquid two-phase flow in pipes, 1st ed. Society of Petroleum Engineers, Richardson.

Taitel, Y., Barnea, D., 1990a. Two-Phase Slug Flow. Adv. Heat Transf. 20, 83–132. doi:10.1016/S0065-2717(08)70026-1

Taitel, Y., Barnea, D., 1990b. A consistent approach for calculating pressure drop in inclined slug flow. Chem. Eng. Sci. doi:10.1016/0009-2509(90)87113-7

Théron, B., 1989. Ecoulements diphasiques instationnaires en conduite horizontale. Institut National Polytechnique de Toulouse, France.

Woods, B.D., Hanratty, T.J., 1996. Relation of slug stability to shedding rate. Int. J. Multiph. Flow 22, 809–828. doi:10.1016/0301-9322(96)00028-6

Yoshizawa, C.J., 2005. Estudos de modelos para a forma das bolhas em um escoamento intermitente padrão golfadas. Universidade Federal do Paraná.

Zabaras, G.J., 2000. Prediction of Slug Frequency for Gas/Liquid Flows. SPE J. doi:10.2118/65093-PA

8. RESPONSIBILITY NOTICE

The authors are the only responsible for the printed material included in this paper.